Nucleic Acids Research, 1998, Vol. 26, No. 14 3379–3384

Allosteric regulation of a ribozyme activity through ligand-induced conformational change

Michihiro Araki, Yasushi Okuno, Yuji Hara and Yukio Sugiura*

Institute for Chemical Research, Kyoto Universitiy, Uji, Kyoto 611-0011, Japan

Received March 31, 1998; Revised and Accepted May 25, 1998

ABSTRACT

An allosteric ribozyme has been designed using the hammerhead ribozyme as the active site and a flavin-specific RNA aptamer as a regulatory site. We constructed six variants with a series of base pairs in the linker region (stem II). Under single turnover conditions, kinetic studies were carried out in the absence and presence of flavin mononucleotide (FMN). Interestingly, FMN addition did not influence the cleavage rate of constructs with a 5–6 bp linker but stimulated the catalytic activity of those bearing a shorter linker. In particular, the apparent k_{cat} of Rz3 increases by ~10-fold upon addition of saturating amounts of FMN. To determine the rate constants ($K_{m'}$ and k_{cat}), the ribozyme regulated most effectively by FMN was further investigated. FMN mainly affected the k_{cat} value, reflecting the rate limiting conformational change step of the overall cleavage reaction, depending on helix formation in stem II. Probably, FMN influences the orientation of structures necessary for the cleavage reaction through stem II formation. The result of chemical modification revealed that binding of FMN to the aptamer domain induced the helix formation in stem II required for catalytic activity. Therefore, a specific FMN-mediated allosteric interaction seems to promote a conformational alteration from an open to a closed structure in stem II. The concept of conformational modification in the allosteric effect is consistent with other allosteric enzymes, suggesting that such a conformational change is a fundamental feature of allosteric enzymes in biological systems.

INTRODUCTION

In metabolic pathways, the catalytic activities of enzymes are enhanced or inhibited by allosteric ligands. Most allosteric enzymes found in nature are oligomers and involve ligand binding sites that can specifically recognize effector molecules. Effector binding to the allosteric binding sites results in allosteric interactions in the tertiary and quaternary structures, inducing a conformational change from an open to a closed structure. Domain closure often helps in positioning of catalytic groups for activity of the enzyme (1). Such allosteric regulation is applicable to a monomer enzyme in the context of interdomain interactions instead of subunit interactions. However, few models have studied allosteric regulation in protein enzymes because of the structural diversity and difficulty in designing an allosteric enzyme.

Some RNA tertiary structures, for example the hammerhead ribozyme and group I intron fragment, have emerged with the development of high resolution RNA structural analysis, using both X-ray crystallography and nuclear magnetic resonance (NMR) spectroscopy (2–4). Molecular recognition between RNA and its specific ligands has also been examined by high resolution NMR on *in vitro* selected RNA–ligand complexes. Indeed, binding of ligands to RNA not only induces a conformational change, but also stabilizes extensive tertiary interactions (5–7). These understandings could provide the information for rational design of a new generation of RNA molecules (8). When the structural and functional potentials are given, a ribozyme can be regulated allosterically with ligand molecules. Although rational design of an allosteric ribozyme controlled by ATP (9) and an allosteric ribozyme designed by *in vitro* selection (10) were recently reported, more detailed analysis is necessary to understand allosteric regulation dependent on conformational modification induced by ligand molecules.

Unlike proteins, RNA has a paucity of primary structure diversity, with only four side chains. The side chains divide into two classes, purines and pyrimidines. Each is a planar group with hydrogen bond donors and acceptors, whereas the protein side chains comprise hydrophobic, hydrophilic and charged groups of various sizes and shapes. The secondary structure of an RNA molecule depends on simple duplex behavior and the energetics of Watson–Crick base pairing interactions. These features are of great advantage to kinetic and structural investigations of allosteric regulation. In fact, the kinetic properties of the hammerhead ribozyme have been understood by measuring individual elementary rate constants based on the duplex behavior (11–13). In addition, chemical probing analysis can conveniently detect the approximate orientation of nucleotides in certain states of variable conformations and also determine the key nucleotides regulating the activities of ribozymes.

In order to obtain a general insight into allosteric regulation, we designed a new allosteric ribozyme containing the hammerhead ribozyme as the active site and a flavin-specific RNA aptamer as a regulatory site. Both the site structures have been highly resolved by X-ray and NMR studies (2,3,14). Kinetic studies and chemical modification experiments were performed in the absence and presence of flavin mononucleotide (FMN). The results indicate that the cleavage activity of certain ribozymes is allosterically enhanced by binding of FMN and that specific FMN binding contributes to the formation of adequate structure for activity through a conformational change in the linker region stem II.

*To whom correspondence should be addressed. Tel: +81 774 38 3210; Fax: +81 774 32 3038; Email: sugiura@scl.kyoto-u.ac.jp

MATERIALS AND METHODS

RNA preparations

Each ribozyme was prepared by *in vitro* transcription from a synthetic DNA template using T7 RNA polymerase, as previously described (15). RNA was purified by electrophoresis through 10% denaturing polyacrylamide–urea gels (PAGE), visualized by UV shadowing, excised and eluted overnight at room temparature in 500 mM ammonium acetate and 1 mM EDTA. The eluates were extracted with 1-butanol and then ethanol precipitated. RNA pellets were washed with 70% ethanol, dried, resuspended in water and quantified by measuring absorbance at 260 nm. The RNA substrate was prepared by standard solid phase methods. Substrate RNA was purified by PAGE, isolated by crush soaking, 5′-^{32}P-end-labeled with T4 polynucleotide kinase and [γ-^{32}P]ATP and repurified by PAGE.

Ribozyme activity assays

Single turnover experiments were performed under conditions of excess ribozyme (final concentration 10–250 nM) over substrate (final concentration 0.5–10 nM). Ribozyme and substrate were separately denatured for 1 min at 90°C in 50 mM Tris–HCl (pH 8.0) containing 100 mM NaCl and cooled at room temperature for 15 min. Each solution containing 10 mM $MgCl_2$ was incubated at 37°C for 15 min in the absence and presence of 100 μM flavin mononucleotide (FMN). The FMN reaction was carried out in the dark to avoid photocleavage (16) and the reactions were initiated by mixing two sample solutions. Aliquots of the reaction mixture were removed at appropriate intervals and quenched with an equal volume of 100 mM EDTA, 9 M urea, 10% glycerol, 0.1% xylene cyanol, 0.1% bromophenol blue. The extents of cleavage were analyzed by 20% PAGE and detected by autoradiography. Apparent cleavage rates (k_{obs}) were obtained from the slopes in semi-logarithmic plots (logarithm of unreacted fraction versus time). In each FMN-dependent experiment, the rate constant was determined similarly, except for addition of 100 μM FMN. The k_{obs} values were evaluated from three independent experiments. In certain cases, ribozyme and substrate were heated and cooled in the buffer and the reaction was initiated by addition of $MgCl_2$ to 10 mM concentration.

In single turnover experiments with increasing FMN concentrations, Rz3 was regulated most effectively by FMN. This system is comprised of the model shown in Scheme 1.

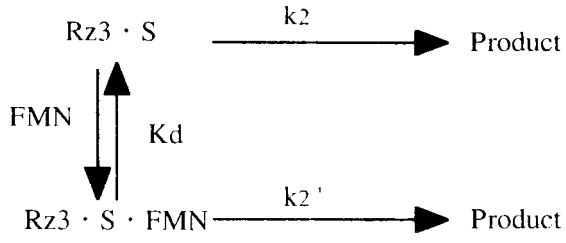

Scheme 1.

K_d is the dissociation constant of FMN from the Rz3–substrate–FMN complex. The values k_2 and $k_{2'}$ are the rate constants for cleavage in the absence and presence of bound FMN respectively (17). The relation between the rate constant k_{2obs} obtained from the single turnover reaction in the presence of FMN and the rate constants k_2 and $k_{2'}$ can be written as follows.

$$k_2[\mathrm{Rz3{\cdot}S}] + k_{2'}[\mathrm{Rz3{\cdot}S{\cdot}FMN}] = k_{2obs}([\mathrm{Rz3{\cdot}S}] + [\mathrm{Rz3{\cdot}S{\cdot}FMN}])$$

$$K_d = \frac{[\mathrm{Rz3 \cdot S}][\mathrm{FMN}]}{[\mathrm{Rz3 \cdot S \cdot FMN}]}$$

By insertion and setting of the equilibrium equation, equation **1** is derived.

$$k_{2obs} = \frac{k_2 \times K_d + k_{2'} \times [\mathrm{FMN}]}{K_d + [\mathrm{FMN}]} \qquad \mathbf{1}$$

The k_{2obs} values obtained at a series of FMN concentrations were fitted to equation **1** by non-linear least squares.

Dimethyl sulfate (DMS) probing assays

After denaturation at 90°C for 1 min, 5′-^{32}P-end-labeled ribozymes were renatured in the absence and presence of 100 μM FMN for 30 min on ice. The sample solution contained 50 mM Tris–HCl (pH 8.0), 100 mM NaCl, 10 mM $MgCl_2$ and 5 μg calf thymus DNA. To probe the N7 positions of guanosine, aniline-induced strand scission was performed. DMS modification was carried out by addition of 1 μl DMS, followed by incubation on ice for 10 min. After ethanol precipitation, the modified RNA was dissolved in 10 μl 1 M Tris–HCl (pH 8.2) and incubated with 0.1 M $NaBH_4$ for 20 min on ice in the dark. The RNA was precipitated again and the pellet was incubated in 20 μl aniline/acetic acid buffer (pH 4.5) for 10 min at 60°C in the dark. Products were sequenced by 15% PAGE and visualized by autoradiography.

RESULTS AND DISCUSSION

Introduction of an FMN binding loop into the hammerhead ribozyme

Hammerhead ribozymes that act *in cis* in nature have been converted into *trans*-acting ribozymes (18,19). The engineered ribozyme can specifically cleave the substrate in a multiple turnover manner. The reaction of the hammerhead ribozyme consists of at least three steps: substrate binding, cleavage and product dissociation. Depending on the length of the substrate and the substrate binding sequence (stems I and III), the rate limiting step varies between the chemical cleavage step and the product release step. Previous reports indicated that stems I and III of shorter sizes than 5 bp shift the rate limiting step from the product dissociation step to the chemical cleavage step (11–13). To avoid kinetic complexity, in design of an allosteric ribozyme the bimolecular hammerhead ribozyme Rz0 (20) was utilized as the basis for the design of new constructs (Fig. 1a). In this case, the catalytic activity of the hammerhead ribozyme depends on the size of stem–loop II. Furthermore, it is known that exact orientation of stem II is important for activity and that loop II can be replaced by other structural moieties (2,3,21,22). In order to regulate formation of stem II by structural change in the FMN-specific aptamer, we inserted an extension to stem II in place of loop II (Fig. 1b). The FMN aptamer was previously found to have conformational characteristics involving formation of a short helix of A-U/G-C pairs on ligand binding and specific affinity for FMN (K_d ~500 nM) (23,24). Presumably, specific binding of FMN rescues the helix formation in stem II which was desrupted by introduction of the FMN binding loop.

Because helix stability in stem II is responsible for overall stability and activity of the ribozyme, alterations in the stem II

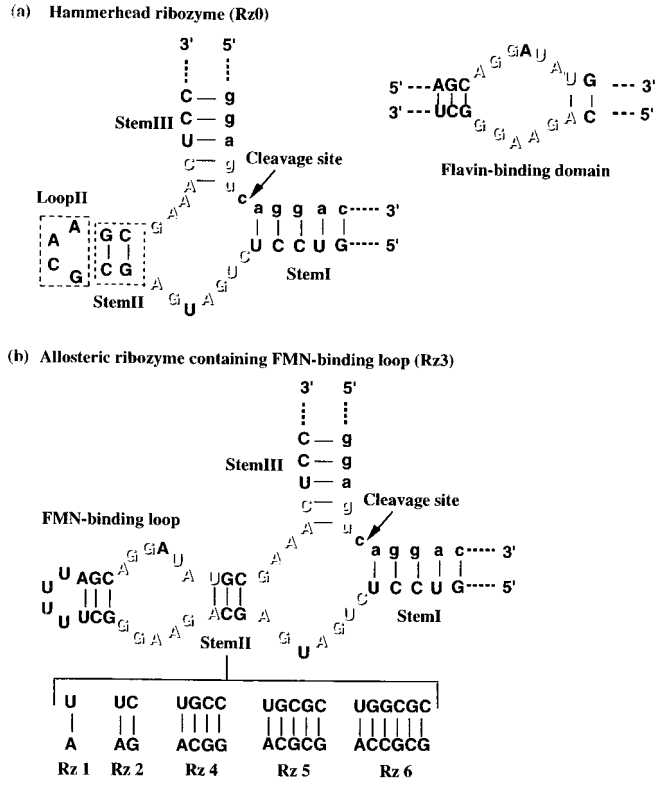

Figure 1. Secondary structures of the native hammerhead ribozyme and designed constructs. (**a**) (Left) Secondary structure of the native hammerhead ribozyme. Outlined residues represent the conserved core sequence. The arrow indicates the position of cleavage. The boxed regions are loop II and stem II of the native ribozyme (Rz0), to be replaced with Rz1–6. (Right) RNA aptamer for specific recognition of FMN. Conserved nucleotides are outlined. (**b**) Sequences of the allosteric ribozyme containing a flavin binding loop with 3 bp of stem II, termed Rz3. Constructs Rz1–6 are modified versions of Rz3 that include base pair variations in stem II. The substrate binding regions (stems I and III) are 11 bp in Rz0–6.

sequence significantly affect catalytic activity of the hammerhead ribozyme (20,25). Six ribozyme constructs with a series of base pairs in stem II were prepared and the cleavage reaction was performed under single turnover conditions. Table 1 summarizes the first order rate constants for substrate cleavage in the ribozyme–substrate complex in the absence and presence of FMN. In Rz0, without a FMN binding site, addition of FMN gave no positive effects. Therefore, it is evident that rate enhancement for the designed ribozyme arose as a result of FMN binding. Compared with Rz0, the rate constant decreased as the number of base pairs in stem II diminished (Rz1–4). In general, a loop configuration destabilizes double helical stem structures in stem–loop regions (26). Thus, introduction of a FMN binding loop was considered to disrupt helix formation in stem II and also to cause loss of the intrinsic catalytic activity in the cases of the variants Rz1–4 with shorter stems II. As clearly shown in Table 1, these chimeric ribozymes were stimulated ~2–6-fold by the presence of FMN. This suggests that FMN helps to stabilize the FMN binding loop and the stem II structure required by the transition state. On the other hand, ribozymes with longer stems II than 5 bp showed high catalytic activities comparable with the activity of Rz0 (Rz5 and Rz6). The activities of Rz5 and Rz6 were unchanged in spite of exogenous addition of FMN, because a longer stem II region would stabilize the helix structure, shielding it from the loop destabilizing effect. Ribozymes possessing stable stems II do not require the stabilizing effect of FMN for an active structure. Therefore, the helix stability of stem II results in important effects not only on the activity of the constructs but also on regulation by FMN. Ribozymes containing a lengthened stem II have an intrinsically high catalytic efficiency without FMN and hence activity would bear no relation to the steric factor of stem I–stem II interaction. In the case of ribozymes with short stems I and III, ribozyme activity is known to depend on the sizes of stem II and loop II. Native ribozymes give high catalytic activity even with 2 bp in stem II, whereas our designed ribozymes require 6 bp as stem II. Therefore, it is difficult to simply compare the catalytic activities of Rz1–6 with those of a control Rz bearing the same linker region but lacking the FMN binding site. As well as FMN, flavin adenine dinucleotide (FAD) also enhanced the catalytic activity of the designed ribozymes. This result is reasonable, because both flavin derivatives can specifically bind to the aptamer by their isoalloxazine ring.

Table 1. Cleavage rate of each ribozyme construct[a]

Ribozyme	k_{obs} (min^{-1}) None	FMN	k_{rel}[b]
Rz 0	0.53 ± 0.09	0.48 ± 0.15	0.9 ± 0.2
Rz 1	0.0075 ± 0.003	0.021 ± 0.01	2.8 ± 1.1
Rz 2	0.028 ± 0.01	0.055 ± 0.02	2.0 ± 0.8
Rz 3	0.028 ± 0.005	0.18 ± 0.07	6.3 ± 0.4
Rz 4	0.15 ± 0.04	0.39 ± 0.09	2.3 ± 0.6
Rz 5	0.39 ± 0.13	0.42 ± 0.08	1.1 ± 0.2
Rz 6	0.35 ± 0.12	0.31 ± 0.11	0.9 ± 0.3

[a]For conditions of single turnover experiments, see Materials and Methods.
[b]The value of k_{rel} shows the rate enhancement of each ribozyme.

Evidence for an allosteric effect of FMN on Rz3

Although single turnover experiments were performed under conditions of a saturating amount of ribozyme, it is uncertain whether FMN affects either k_{cat} or $K_{m'}$. We determined the rate constants for the cleavage reaction with Rz3, possessing the most effective FMN switch function. Because (i) the reaction did not follow a Michaelis–Menten kinetic scheme (data not shown) and (ii) distinction between the first and second turnover phases is difficult in experiments with excess substrate, the cleavage rate constant was determined from a pseudo-first order reaction using a trace amount of radioactive substrate and various concentrations of ribozyme in excess over substrate (18). The single turnover rates were plotted as a function of ribozyme concentration in Eadie–Hofstee plots and then k_{cat} and $K_{m'}$ values were obtained from the *y*-intercept and the slope respectively (Table 2). The half maximal concentration of the reaction velocity was termed $K_{m'}$, since it is not a true Michaelis–Menten parameter. The incorporation of a FMN binding domain gave $K_{m'}$ and k_{cat} values of 93 nM and 0.024/min respectively. In the presence of FMN, the $K_{m'}$ value was almost unchanged and a 10-fold increase in $k_{cat}/K_{m'}$ was observed as a result of a rise in the rate constant k_{cat}. The $K_{m'}$ value is representative of the affinity between ribozyme and substrate,

indicating that FMN does not influence the substrate binding step. On the other hand, two hypothetical steps of the kinetic mechanism determine the k_{cat} value, which reflects the rate limiting step of the reaction, namely the chemical cleavage step and the conformational change step. In our constructs, the latter step contributes more to the rate limiting step, because introduction of a FMN binding loop probably causes misfolding and deformation in the catalytic core. Presumably, the allosteric effect of FMN could overcome the conformational change step limiting the reaction rate. The catalytic activities of the designed ribozymes appear to be lower than those of native ribozymes under similar conditions. For ribozymes with short arms I and III, k_{cat} is usually between 1 and 4 min at pH 7.4.

Table 2. Kinetic parameters for Rz3[a]

Ribozyme	FMN	$K_{m'}$ (nM)	k_{cat} (min^{-1})	$k_{cat}/K_{m'}$ ($\mu M^{-1}min^{-1}$)
Rz3		93 ± 30	0.024 ± 0.016	0.26 ± 0.18
Rz3	100 μM	70 ± 18	0.26 ± 0.05	3.7 ± 1.2

[a]Values obtained from plots of cleavage rates (k_{obs}) versus k_{obs}/[R] in experiments with various concentrations of [R] and trace amounts of [5′-^{32}P]substrate.

Next, a pre-annealing experiment was carried out to confirm the result that FMN does not influence the substrate binding step but the conformational change step prior to the cleavage step (Fig. 2). As expected, exogenous addition of FMN enhanced catalytic activity, although cleavage appeared to level off after only 50% substrate consumption. Addition of FMN during the ribozyme reaction abolished the slow phase observed in the absence of FMN. FMN overcame the slow phase that indicates the rate limiting step. Because the allosteric effect of FMN induces a conformational alteration in the ribozyme, the conformational change step limits the reaction rate. According to the previous model to account for this kinetic mechanism (see Materials and Methods), single turnover experiments were performed in increasing concentrations of FMN. Figure 3 shows the activity curve obtained with each concentration of FMN. Activation of Rz3 by FMN levelled off as the added FMN concentration increased, indicating that FMN saturates its binding site and specific FMN binding enhances the catalytic activity of Rz3. The solid line represents the best fit of the data to equation 1. The estimated K_d value of 129 ± 24 μM differs from the reported K_d of FMN with the aptamer. Probably, the difference is attributed to our FMN binding loop with few base pairs as the FMN aptamer. In addition, the obtained $k_{2'}$ value (0.45/min) is considerably larger than the k_2 value (0.014/min) and is similar to that observed for Rz0. The $k_{2'}$ value reflects the chemical cleavage step, while the k_2 value reflects the conformational change step prior to chemical cleavage. Binding of FMN enhances catalytic activity by rearrangement of the active conformation, the rate limiting step.

Previous X-ray crystal studies of the hammerhead ribozyme clarified the close proximity orientation of stem I and stem–loop II (2,3). Tertiary interaction between stem I and stem–loop II has an essential effect on the catalytic core domain of the ribozyme. Indeed, the cleavage activity of an ATP-responsive ribozyme is inhibited by specific binding of ATP, because of mutually exclusive formation of the ribozyme domain and the ATP–aptamer domain complex located in stem I and stem–loop II respectively (9). Our computer modeling based on the published structures of the hammerhead ribozyme and the FMN–aptamer complex

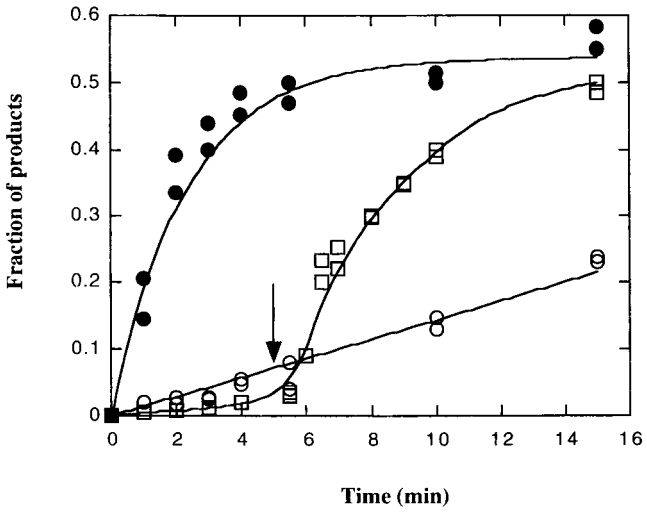

Figure 2. Induction of catalysis during the course of ribozyme reaction in the absence (○) and presence (●) of 100 μM FMN. The 5′-^{32}P-end-labeled substrate was pre-annealed with Rz3 before reaction. FMN was added to a final concentration of 100 μM during an ongoing reaction (□). The arrow indicates the time of FMN addition (5 min).

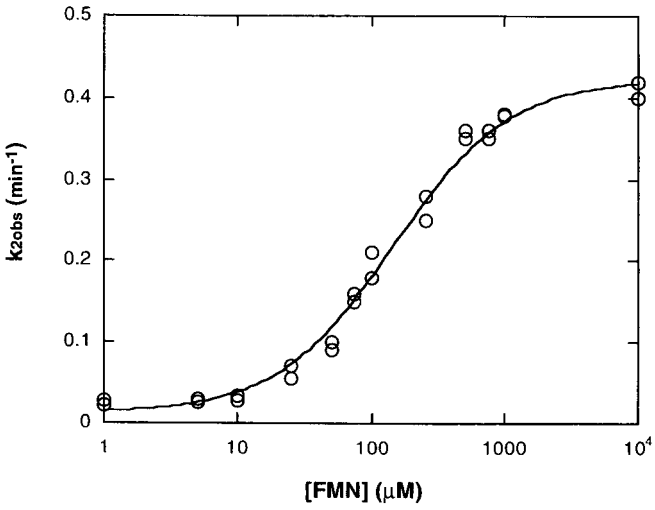

Figure 3. FMN concentration dependence of the observed first order rates of Rz3–substrate complex formation. Single turnover reactions after pre-annealing were carried out at increasing concentrations of FMN. The line indicates the least squares fits of the experimental data to equation **1**.

revealed a spatially separated orientation, indicating that the FMN–loop complex does not interact with stem I (data not shown). Although extensive experiments on the tertiary interaction between the FMN–loop complex and the ribozyme domain are required, our constructs explain positive regulation by induction of the active conformation of the catalytic domain mainly dependent on stem II formation.

Different DMS accessibilities of Rz3 and Rz6

Kinetic evidence indicates that the allosteric effect of FMN on the activity of Rz3 is brought about by a conformational alteration in

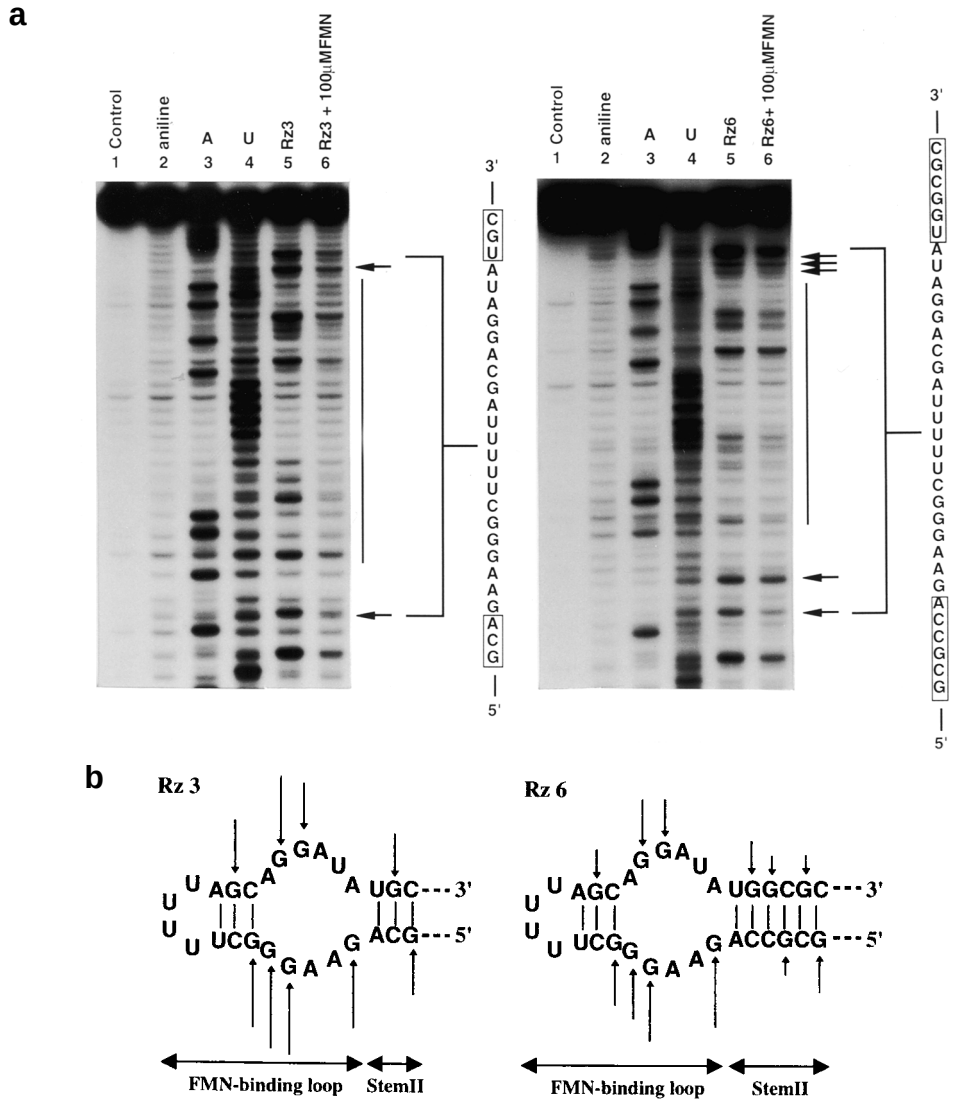

Figure 4. DMS modification experiments of 5′-^{32}P-end-labeled Rz3 and Rz6. (**a**) Autoradiogram of a 15% denaturing gel of the aniline-induced cleavage reaction of DMS-modified Rz3 (left) and Rz6 (right). Lane 1, intact RNA; lane 2, cleavage products from aniline treatment in the absence of DMS; lane 3, A-specific reaction of Rz3 and Rz6; lane 4, U-specific reaction of Rz3 and Rz6; lane 5, cleavage products obtained from DMS-modified Rz3 and Rz6 in the absence of FMN; lane 6, cleavage products obtained from DMS-modified Rz3 and Rz6 in the presence of 100 μM FMN. Boxed regions indicate nucleotides in the stem II region. Arrowheads show guanosines in the stem II region. The line on the right indicates nucleotides in the FMN binding loop. (**b**) Observed differences of cleavage intensities at the indicated guanosines of Rz3 and Rz6 in the absence and presence of FMN. Arrow lengths are proportional to the extent of the cleavage difference.

the ribozyme, especially by formation of a stable stem II moiety. FMN had no positive effects on Rz6, with a longer stable stem II, presumably because stem II itself forms an adequate structure for catalysis and the conformational change step observed in Rz3 may not exist (Table 1). To determine whether the conformational alteration in stem II resulting from FMN binding relates to ribozyme activity, DMS modification was carried out for Rz3 and Rz6 with or without FMN. This probe specifically modifies position N7 of guanosine in Watson–Crick pairings, in particular the base site in the unpaired state. If helix formation in stem II is induced by addition of FMN, DMS accessibility to stem II would decrease. DMS modification was performed on ice, because the ribozyme forms a stable complex with FMN at lower temperatures.

No detectable changes were observed for Rz0 in spite of addition of FMN (data not shown). In free Rz3, every guanosine within the FMN binding loop (line) and stem II (arrow) was accessible for DMS modification (Fig. 4a), indicating that introduction of the FMN binding loop spreads out the overall structure to disrupt formation of stem II. In the presence of FMN, a reduced intensity of the corresponding modification bands was clearly detected, not only in the FMN loop but also in the stem II region (Fig. 4b). Complex formation with the FMN binding loop contributes to formation of stem II. This conformational change would have a serious effect on the catalytic activity of Rz3. In the case of free Rz6, the guanosines in the FMN binding loop and stem II were less accessible to DMS, suggesting that the stem II moiety of Rz6 alone originally forms a stable helix (6 bp) and that its whole structure is also in a closed state (Fig. 4a). In the presence of FMN, the band intensity of the FMN binding loop region was reduced to 70–90% of that observed in Rz3. Although

FMN surely binds the FMN binding loop site, inducing formation of a FMN–loop complex, the stem II region was almost unchanged except for the guanosines on the edge of stem II (Fig. 4b). Other guanosine residues within stems I and III seem to be insensitive to the presence of FMN. The difference in DMS accessibility of the stem II region between Rz3 and Rz6 corresponds well with the kinetic results. In Rz3, the conformational change process exists as the rate limiting step of the reaction. The structural alteration caused by FMN overcomes this rate limiting of the reaction and produces a high catalytic efficiency. However, the effect of FMN is not essential for Rz6, since this construct itself has high activity without structural alteration and the conformational change step virtually does not exist in the kinetic scheme. Ribozyme activity depends significantly on helix formation in stem II and also the extent of the FMN effect is due to whether the stem II region is in an open or closed state. These results provide insights into the molecular basis of allosteric regulation of ribozymes and such a regulatable ribozyme may have applicability in future gene therapy strategies.

CONCLUSION

To examine the allosteric regulation of ribozyme activity, we designed and constructed an allosteric ribozyme consisting of the hammerhead ribozyme and a flavin-specific RNA aptamer. Rz3, with 3 bp in stem II, was most effectively regulated by FMN. FMN binding affects the rate limiting conformational change step of the overall cleavage reaction rather than the substrate binding step, indicating that FMN binding contributes to the formation of a necessary conformation for catalytic activity through stem II formation. DMS probing analysis also supports a FMN-mediated allosteric interaction between the ribozyme and aptamer domains. This allosteric effect promotes a conformational alteration from open to closed structures in stem II. On the basis of our models, it is possible to engineer the hammerhead ribozyme to give an allosteric ribozyme which has a conformational transition in common with other allosteric enzymes. The present study provides evidence that ligand molecules can exert an allosteric effect on ribozyme-catalyzed reactions beyond conformational changes and structural stabilization.

ACKNOWLEDGEMENTS

This study was supported in part by a Grant-in-Aid for Scientific Research from the Ministry of Education, Science, Sports and Culture, Japan. We are also thankful for a grant from the Fujisawa Foundation.

REFERENCES

1 Gerstein,M., Lesk,A.M. and Chothia,C. (1994) *Biochemistry*, **33**, 6739–6749.
2 Pley,H.W., Flaherty,K.M. and McKay,D.B. (1994) *Nature*, **372**, 68–74.
3 Scott,W.G., Murray,J.B., Arnold,J.R.P., Stoddard,B.L. and Klug,A. (1996) *Science*, **274**, 2065–2069.
4 Cate,J.H., Gooding,A.R., Podell,E., Zhou,K., Golden,B.L., Kundrot,C.E., Cech,T.R. and Doudna,J.A. (1996) *Science*, **273**, 1678–1699.
5 Patel,D.J., Suri,A.K., Jiang,F., Jiang,L., Ajay Kumar,P.F.R. and Nonin,S. (1997) *J. Mol. Biol.*, **272**, 645–664.
6 Chow,C.S. and Bogdan,F.M. (1997) *Chem. Rev.*, **97**, 1489–1513.
7 Jenison,R.D., Gill,S.C., Pardi,A. and Polisky,B. (1994) *Science*, **263**, 1425–1429.
8 Breaker,R.R. and Joyce,G.F. (1994) *Trends Biotechnol.*, **12**, 268–275.
9 Tang,J. and Breaker,R.R. (1997) *Chem. Biol.*, **4**, 453–459.
10 Tang,J. and Breaker,R.R.(1997) *RNA*, 3, 914–925.
11 Ruffner,D.L., Stormo,G.D. and Uhlenbeck,O.C. (1990) *Biochemistry*, **29**, 10695–10702.
12 Fedor,M.J. and Uhlenbeck,O.C. (1992) *Biochemistry*, **31**, 12042–12054.
13 Hertel,K.J., Herschlag,D. and Uhlenbeck,O.C. (1994) *Biochemistry*, **33**, 3374–3385.
14 Fan,P., Suri,A.K., Fiara,R., Live,D. and Patel,D.J. (1996) *J. Mol. Biol.*, **258**, 480–500.
15 Milligan,J.F. and Uhlenbeck,O.C. (1989) *Methods Enzymol.*, **180**, 51–62.
16 Burgstaller,P. and Famulok,M. (1997) *J. Am. Chem. Soc.*, **119**, 1137–1138.
17 Peracchi,A., Beigelman,L., Usman,N. and Herschlag,D. (1996) *Proc. Natl. Acad. Sci. USA*, **93**, 11522–11527.
18 Uhlenbeck,O.C. (1987) *Nature*, **328**, 596–600.
19 Haseloff,J. and Gerlach,W.L. (1988) *Nature*, **334**, 585–591.
20 Tuschl,T. and Eckstein,F. (1993) *Proc. Natl. Acad. Sci. USA*, **90**, 6991–6994.
21 Symons,R.H. (1992) *Annu. Rev. Biochem.*, **61**, 641–671.
22 Fu,D., Benseler,F. and Mclaughlin,L.W. (1994) *J. Am. Chem. Soc.*, **116**, 4591–4598.
23 Burgstaller,P. and Famulok,M. (1994) *Angew. Chem. Int. Edn English*, **33**, 1084–1087.
24 Burgstaller,P. and Famulok,M. (1996) *Bioorg. Med. Chem. Lett.*, **6**, 1157–1162.
25 McCall,M.J., Hendry,P. and Jennings,P.A. (1992) *Proc. Natl. Acad. Sci. USA*, **89**, 5710–5714.
26 Turner,D.H., Sugimoto,N. and Freier,S.M. (1988) *Annu. Rev. Biophys. Biophys. Chem.*, **17**, 167–192.